AER/AGS Information Series 148

Alberta Energy Regulator

# Examples of Landslides and the Geological, Topographic, and Climatic Factors That Contribute to Landslide Susceptibilities in Alberta: A Cross-Reference to the Explanatory Notes for AGS Map 605

AGS
ALBERTA GEOLOGICAL SURVEY

**AER/AGS Information Series 148**

# Examples of Landslides and the Geological, Topographic, and Climatic Factors That Contribute to Landslide Susceptibilities in Alberta: A Cross-Reference to the Explanatory Notes for AGS Map 605

S.M. Pawley, G.M.D. Hartman and D.K. Chao

Alberta Energy Regulator
Alberta Geological Survey

February 2017

ISBN 978-1-4601-0167-4



Pawley, S.M., Hartman, G.M.D. and Chao, D.K. (2017): Examples of landslides and the geological, topographic, and climatic factors that contribute to landslide susceptibilities in Alberta: a cross-reference to the explanatory notes for AGS Map 605; Alberta Energy Regulator, AER/AGS Information Series 148, 26 p.

**Published February 2017 by:**
Alberta Energy Regulator
Alberta Geological Survey
4th Floor, Twin Atria Building
4999 – 98th Avenue
Edmonton, AB T6B 2X3
Canada

Tel: 780.638.4491
Fax: 780.422.1459
E-mail: AGS-Info@aer.ca
Website: ags.aer.ca

# Contents



# Tables



# Figures

## Acknowledgements

We thank the following people and organizations:

- R. Skirrow and R. Wang from Alberta Transportation for external science review
- Alberta Energy Regulator staff C.R. Froese, N. Atkinson, and T. Shipman for technical review; L.D. Andriashek, M. Grobe, D.I. Pană, T.E. Hauck, and B. Hathway for geological assessment; K. Mckay for GIS cartography; and D. Wood and J. Slomka for graphic design

## Abstract

This document highlights the common landslide types and examples in the Alberta Plains. It also describes the degree to which terrain can be affected by landslides by modelling a relationship between the spatial distribution of recognized landslides, and predisposing geological, topographic, and climate factors .

The content of this document is cross-referenced to the explanatory notes for the Relative Landslide Susceptibility Model of the Alberta Plains and Shield Regions (AGS Map 605).

A 2-page printable version of the AGS Map 605 at 1:1 000 000 scale and explanatory notes in PDF format (32 x 50 inches per page) and the model result as gridded data (DIG 2016-0044) can be downloaded at no charge from the Alberta Geological Survey website.

# 1 Introduction

The evaluation methodology does not assess the effect of significantly folded and faulted bedrock structure, and therefore does not include the mountains and foothills physiographic regions, where bedrock structure is the main geological control on landslide susceptibility (Mollard, 1977). While bedrock structure within the Canadian Shield is complex, it is not considered a significant geological control on landslide susceptibility due to the high strength of bedrock in that region; therefore, the Canadian Shield has been included in the model.

AGS Map 605 (Figure 2; Pawley et al., 2016) represents a predictive statistical model of landslide susceptibility of the Alberta portion of the Interior Plains and Canadian Shield (Figure 1; Bostock, 2014). The model predicts the degree to which terrain can be affected by landslides based on a statistical procedure that establishes a relationship between the spatial distribution of recognized landslides, and predisposing geological, topographic, and climatic factors (Brabb, 1984).

The map portrays the spatial distribution of landslide susceptibility across the Alberta Plains as a relative ranking from low to high. This map does not depict the distribution of known landslides, but identifies landslide-susceptible terrain. Neither does it evaluate the probability of landslide occurrence over any specific period of time (Parise, 2001), nor does it evaluate the magnitude or impact of any potential landslide activity. Consequently, the map should not be interpreted for the purpose of site-specific landslide identification, landslide activity assessment, or landslide hazard appraisal. It is intended to be used only for informational purposes at the regional scale.

# 2 Landslide Definition and Classification

The term "landslide" is defined here as the mass movement of rock, debris, or earth down a slope (Cruden, 1991), and is identified by the movement itself, as well as the resultant landform (Highland and Bobrowsky, 2008). Sinkholes and collapse structures are not considered landslides. Furthermore, our evaluation is intended to predict the landslide susceptibility on natural slopes, not on engineered slopes.

Cruden and Varnes (1996) classified landslides according to their constituent material and the type of movement. Material classification includes rock, earth, and debris where "rock" refers to hard or firm material that was intact and in its natural position before landslide initiation; "earth" is comprised of dominantly fine (<2 mm sized) mineral and/or rock particles; and "debris" is comprised of dominantly coarse (>2 mm sized) mineral and/or rock particles. Movement types include: slides and flows (Figure 3 and Figure 4), spreads, falls, and topples. Slides are mass movements along a discrete rupture surface or within thin zones of intense shearing (Cruden

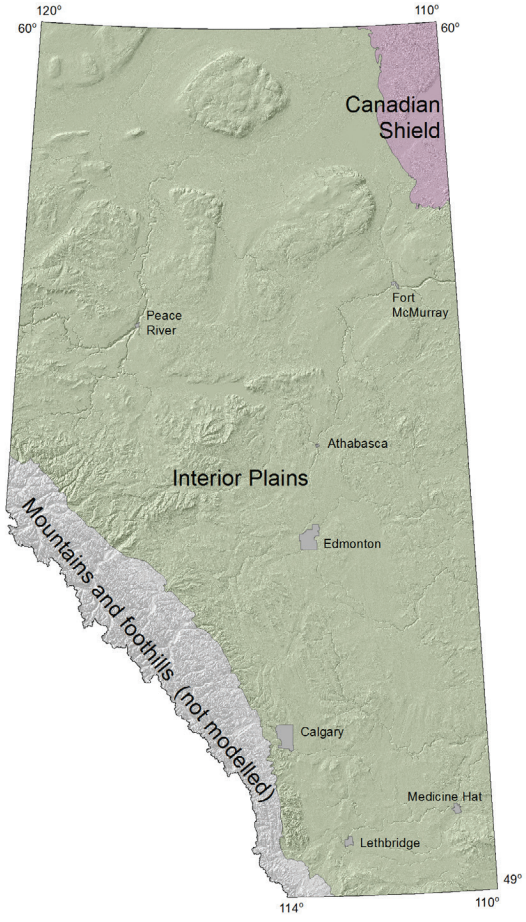


**Figure 1. Physiography of Alberta.**


**Figure 2. AGS Map 605: Relative landslide susceptibility model of the Alberta Plains and shield regions (Pawley et al., 2016).**

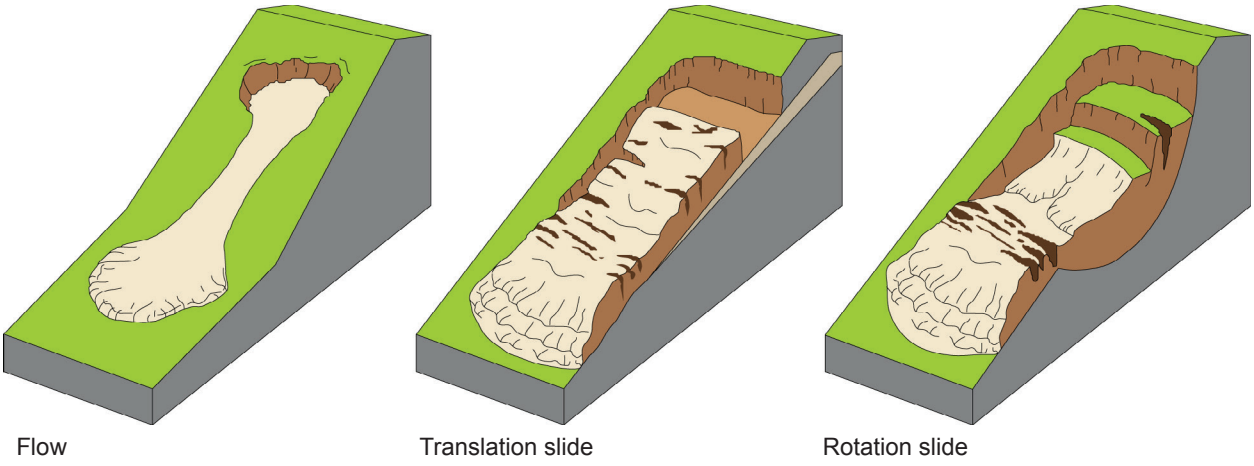


**Figure 3. Landslide type classification (modified from USGS, 2004).**

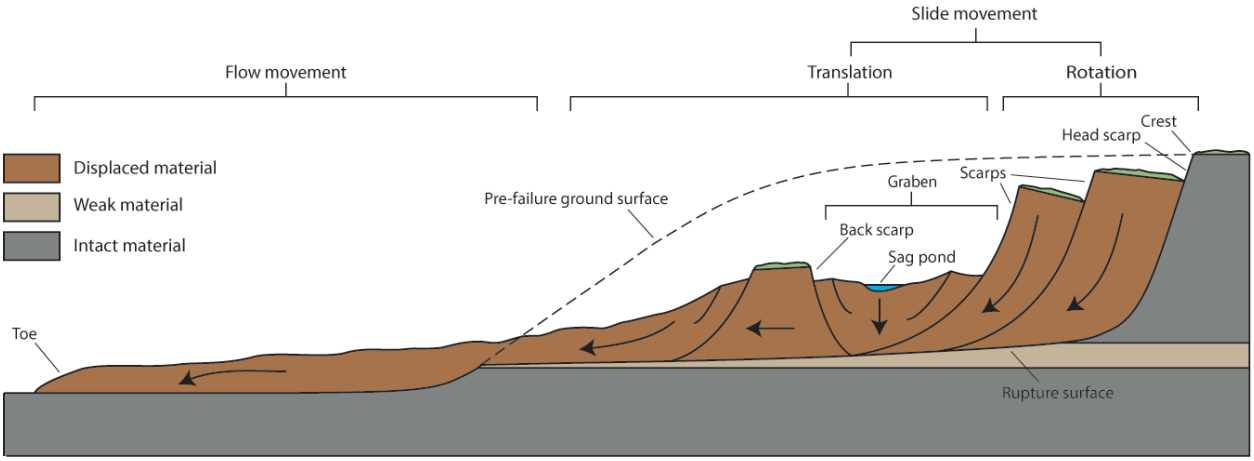


**Figure 4. Schematic cross-section of a composite slide-flow landslide showing displacement vectors and geomorphic features.**

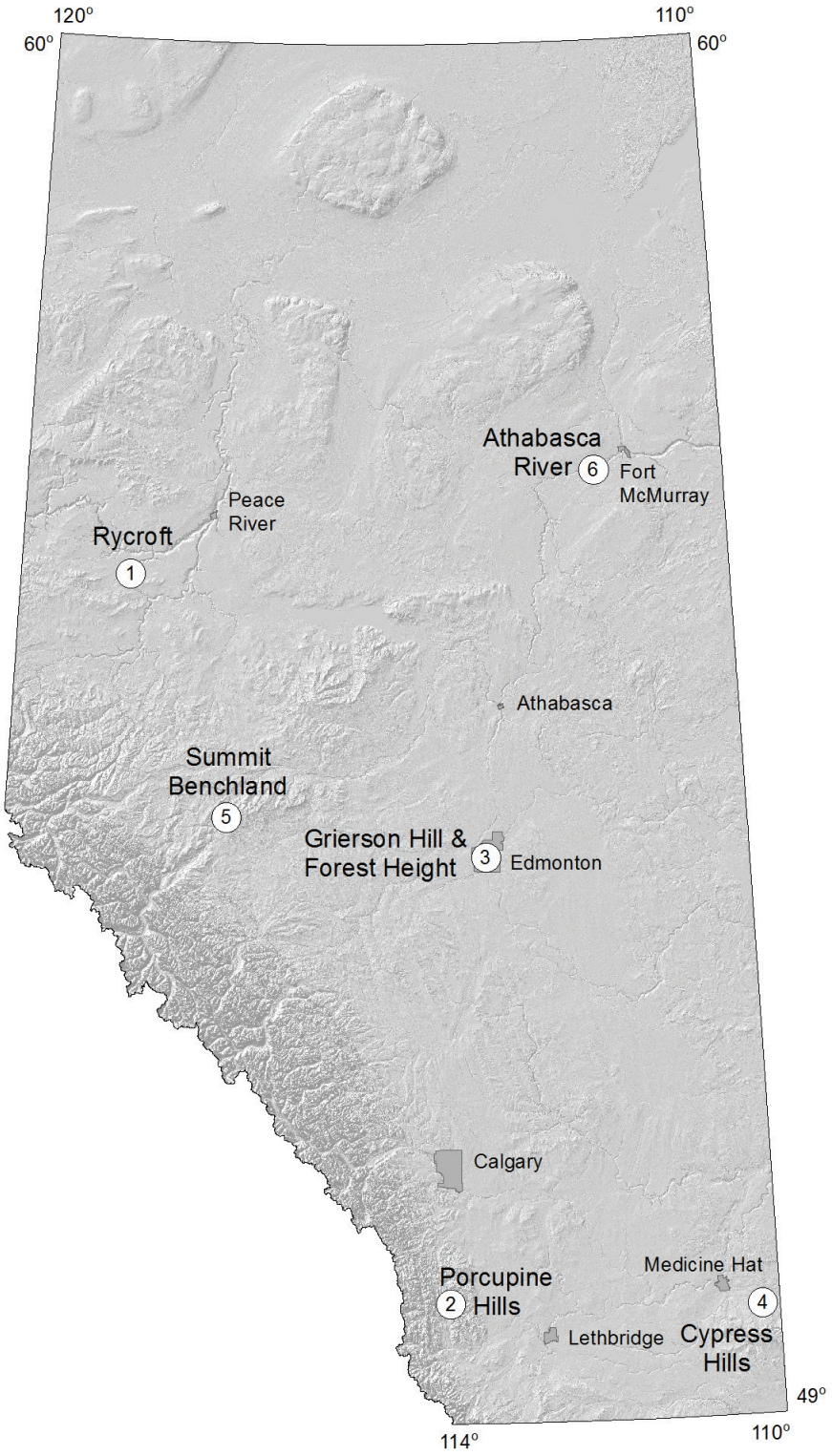


**Figure 5. Locations of landslide examples.**

and Varnes, 1996). Flows are mass movements of liquefied material (Hungr et al., 2001). Composite landslides involve movement which transitions downslope from a slide to a flow. These are the dominant movement types on the Alberta Plains reflecting its physiography and geology. Spreads, falls, and topples are not recognized in this model because they are generally small and uncommon.

## 2.1 Example Landslides of the Alberta Plains

The following examples are representative of the landslides that typically develop within the landslide-susceptible terrain of the Alberta Plains and are recognized in this model (Figure 5). Each landslide is displayed using an image from a hill-shaded bare-earth LiDAR (Light Detection and Ranging) digital elevation model (DEM). LiDAR is particularly effective for landslide mapping because it has the ability to reveal the geomorphology of the 'bare-earth' surface in unprecedented detail, even beneath dense forest cover. The movement type and material of each landslide is classified as per Cruden and Varnes (1996) and includes slide, flow, and composite slide-flow landslides comprised of rock and earth. Slide movement type (Figure 3 and Figure 4) may be recognized by geomorphic features that indicate brittle deformation of material that has slid upon a rupture surface including: tension cracks, scarps and benches, grabens (linear depressions between slide blocks), and sag ponds (water ponded within grabens, upon back-rotated blocks, or behind back scarps). Flow movement type may be recognized by geomorphic features indicative of ductile deformation including globular lobes, compressional ridges, and topographically controlled flows (constriction where confined and spreading where unconfined).

### *2.1.1 Rycroft Landslide*

The Rycroft landslide (Figure 6) occurred in 1990 within the Saddle River valley. The landslide is approximately 980 m wide at its crest, and 100 m in height from crest to toe. Cruden et al. (1993) described the landslide as a reactivated translational earth slide developed within glaciolacustrine clay deposited within a pre-glacial valley. The landslide obstructed the river, forming a dam and impounding a lake. Overtopping of the dam began in spring of 1991 (Cruden et al., 1993). No impoundment is visible on 2014 imagery, suggesting that the dam has been eroded.

### *2.1.2 Slide-Earth Flows at Porcupine Hills*

Two shallow composite rock slide–earth flows converge at the head of Minor Coulee in the dissected upland of the Porcupine Hills (Figure 7). The northern landslide is approximately 630 m wide, 2000 m long, and 275 m in height. The southern landslide is approximately 560 m wide, 1500 m long, and 200 m in height. These landslides developed in weak, bentonitic sandstone-shale within the Porcupine Hills Formation (Jackson, 2002), initiating as rock slides and evolving to earth flows as they propagated downslope.

### *2.1.3 Grierson Hill and Forest Height Landslides*

The Grierson Hill landslide and the Forest Heights landslide (Figure 8, dashed outline in the east) within the City of Edmonton provide examples of translational slides that have exhibited movement for more than 100 years (Cruden et al., 1993; Soe Moe et al., 2009). Both landslides are seated in bedrock, but are comprised of glacial sediments in their upper parts. Both landslides are ultimately caused by erosion at the toe along outside river bends, however, other causal factors include, bentonite seams, coal mining, and elevated groundwater levels. Slope-stabilization efforts and grading have muted the rugged appearance of the Grierson Hill landslide. Both landslides are approximately 50 m in height. The Grierson Hill landslide and the Forest Heights landslide extend along approximately 850 m and 1100 m of riverbank, respectively.

### 2.1.4 Slide-Earth Flow at Cypress Hills

A composite rock slide–earth flow within a ravine on the north flank of the Cypress Hills, 5 km east of Elkwater (Figure 9). The landslide is approximately 1000 m wide, 750 m long, and 90 m in height. Several smaller, secondary earth flows have developed within the lower part of the main landslide. These flows were funnelled toward channels incised within the floor of the ravine. Geomorphologically similar landslides have developed along much of the northwest flank of the Cypress Hills including the Police Point landslides (Sauchyn and Nelson, 1999), forming long contiguous zones of landslide terrain.

### 2.1.5 Slide-Earthflow at Summit Benchland

A composite rock slide–earth flow on the east flank of the Summit Benchland (Pettapiece, 1986; Figure 10). The landslide is approximately 570 m wide, 1540 m long, and 230 m in height. Topographic control of the lower flow component of the landslide is exhibited by its segregation on either side of an intact ridge.

### 2.1.6 Translation Landslide at the Athabasca River Valley

A suite of translational landslides developed within weak rock and earth in the upper slope surrounding an abandoned meander on the north side of the Athabasca River valley, 24 km upstream of Ft. McMurray (Figure 11). Undeformed, horizontally stratified bedrock structure is visible in a consistent mid-slope position indicating that bedrock in the lower portion of the slope is unaffected by landsliding, similar to nearby landslides described by Barlow (2000). Globular earth-flow lobes derived from landslides in the upper part of the slope drape the middle and lower slopes. The slope is approximately 140 m in height.

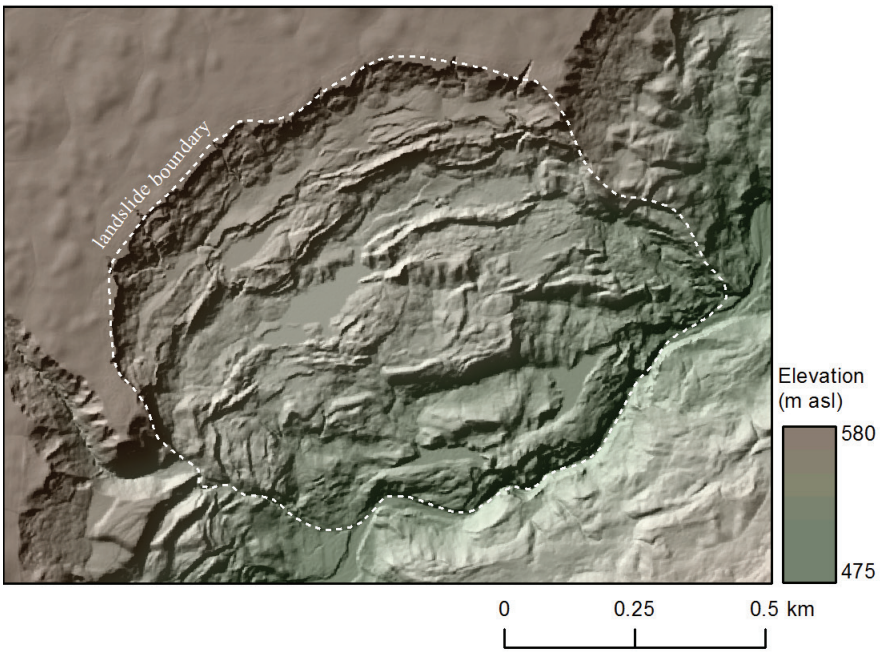


**Figure 6. Rycroft landslide.**

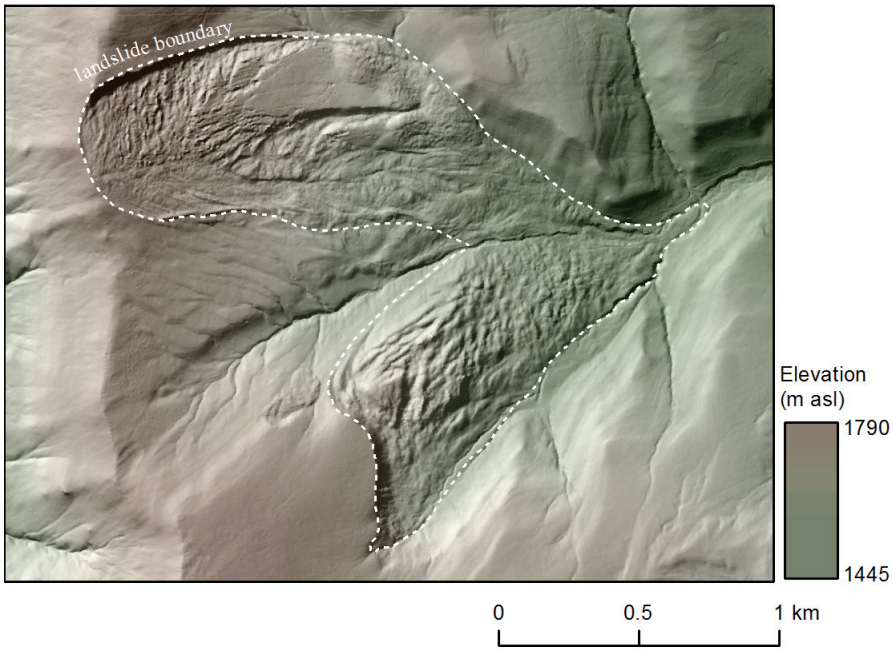


**Figure 7. Slide-earth flows at Porcupine Hills.**


**Figure 8. Grierson Hill and Forest Height landslides.**

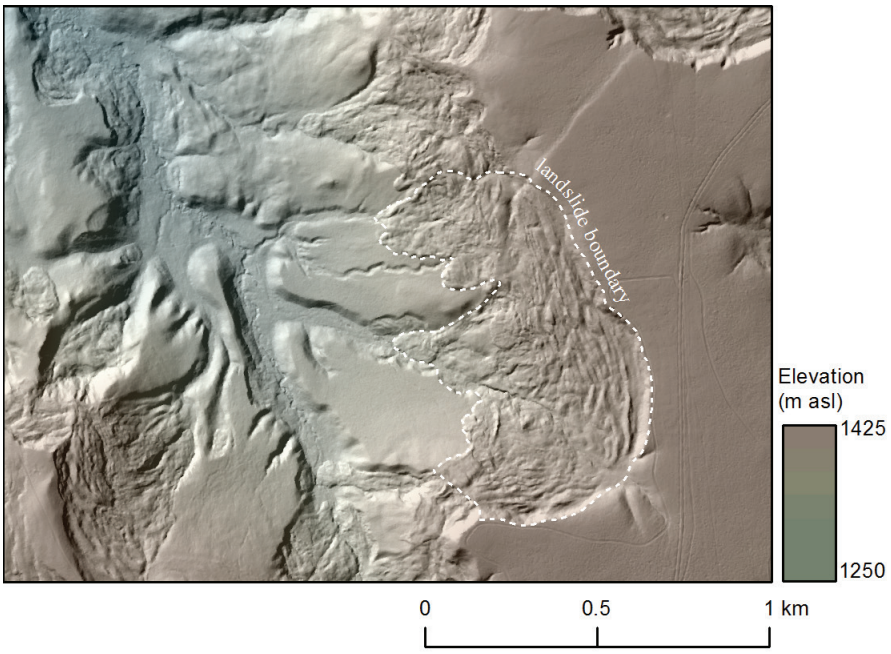


**Figure 9. Slide-earth flow at Cypress Hills.**

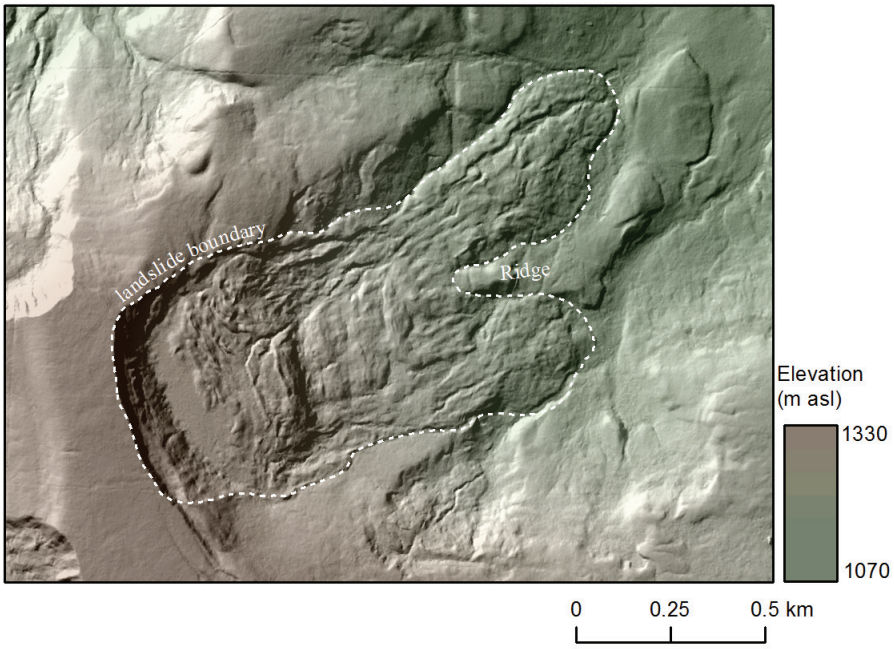


**Figure 10. Slide-earthflow at Summit Benchland.**

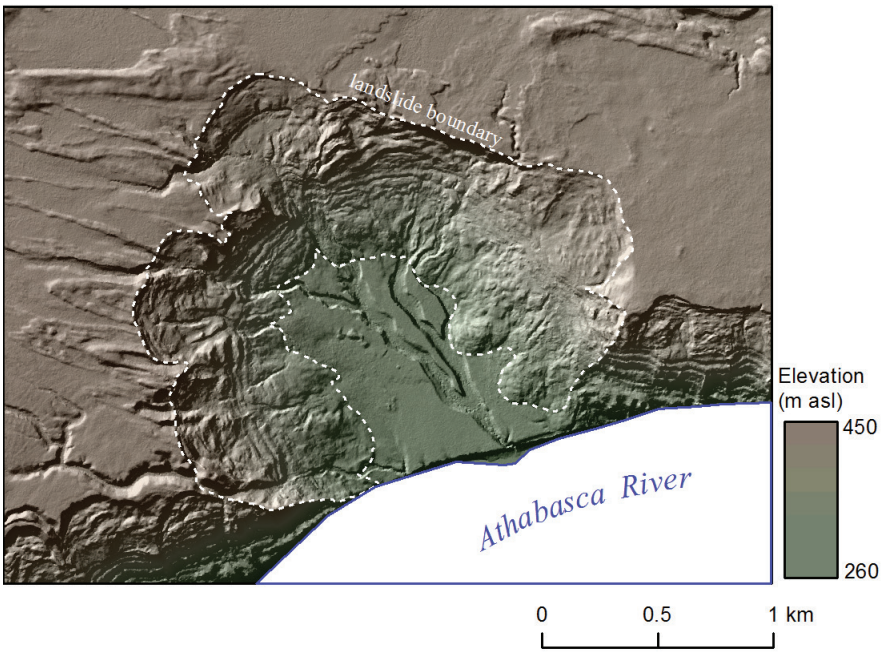


**Figure 11. Translation landslide at the Athabasca River valley.**

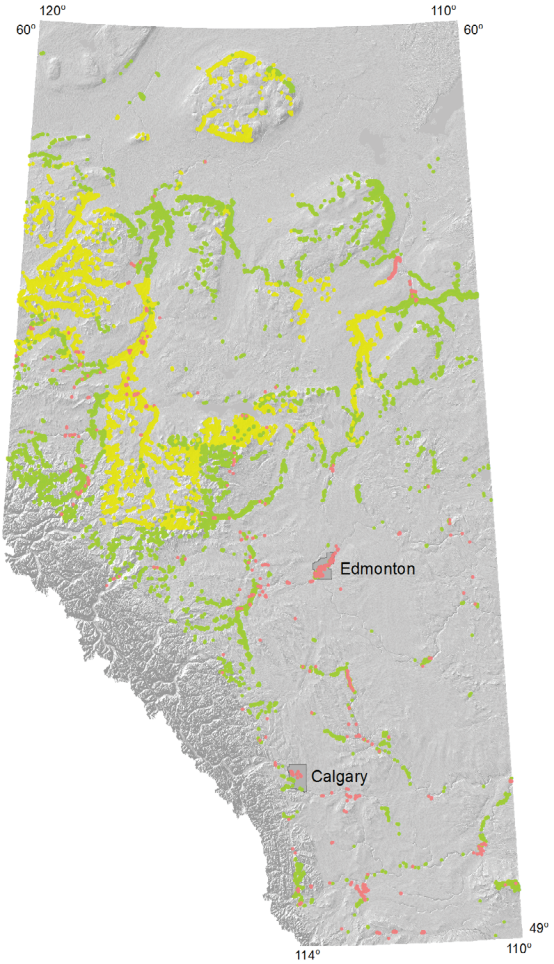


**Figure 12. Data distribution colour coded by data source (see Table 1).**

# 3 Methodology

## 3.1 Landslide Inventory

The landslide susceptibility model uses point-based sampling of landslide and non-landslide terrain. Information regarding landslide distribution was compiled from previously published surficial geology maps, reports, and university theses (Table 1). These sources included polygon data that delineate the extent of mapped landslides, as well as point data that represent single locations within a landslide. The polygon data were converted to points by randomly sampling the landslide polygons with a density of one point per km$^2$. These data were augmented by sampling new landslide features that were mapped from a number of aerial imagery data sources including LiDAR. The final inventory contains ~23,000 points.

**Table 1. Data sources (see Figure 12 for data distribution).**

| Source | Count | Description |
|---|---|---|
| AGS Surficial Geology Maps (Landslide Polygon Features) | 9 364 | Point data converted from polygons (n = 2435) that delineate the outlines of landslide bodies based on airphoto and/or LiDAR imagery interpretation. Polygons were converted to point features using a point density of 1 point per km$^2$. |
| AGS Surficial Geology Maps (Landslide Point Features) | 386 | Point symbols of landslides from published surficial geology maps. Landslides were identified by geologists through field-work or from the interpretation of aerial imagery (airphotos and/or LiDAR data). |
| Published reports | 812 | Point data of landslide locations that were compiled from available engineering reports, journal publications, and university theses. |
| AGS Landslide Locations | 12 628 | Point data of landslide locations from mapping conducted within this project using LiDAR data and high-resolution ortho-imagery. Includes small landslides that were mapped as individual points, and large landslides that were mapped as polygons (n = 2300), which were converted to point data using a point density of 1 point per km$^2$. |

## 3.2 Landslide Predisposing Factors

Landslide susceptibility modelling was performed by assessing the spatial likelihood of landslide occurrence on a cell-by-cell basis relative to predisposing geological, topographic, and climatic factors. A grid-cell resolution of 90 m was found to optimize model performance. In an exploratory analysis, a wide range of landslide predisposing factors were evaluated for their capacity to predictively model the distribution of landslides in the inventory data (Regional-scale landslide susceptibility modelling of Alberta, Canada: comparative results using multiple statistical and machine-learning prediction methods, S.M. Pawley, G.M.D. Hartman and D.K. Chao, work in progress, 2016). The predisposing factors that exert the strongest influence on the landslide susceptibility are outlined here.

### *3.2.1 Local Terrain Morphology*

The Shuttle Radar Topographic Mission (SRTM) DEM (U.S. Geological Survey, 2014) was used to characterize the geomorphological settings associated with landslide-prone terrain. For this purpose, standard morphometric variables consisting of slope angle (Figure 14), aspect, profile curvature, and tangential curvature were calculated from the SRTM DEM (Figure 13). The variability of the terrain, or topographic roughness, is also useful for characterizing landslide morphology, and was evaluated using the Vector Ruggedness Measure (VRM; Sappington et al., 2007) which assesses the variability of slope and aspect simultaneously (Figure 15).


**Figure 13. SRTM DEM (USGS, 2014).**

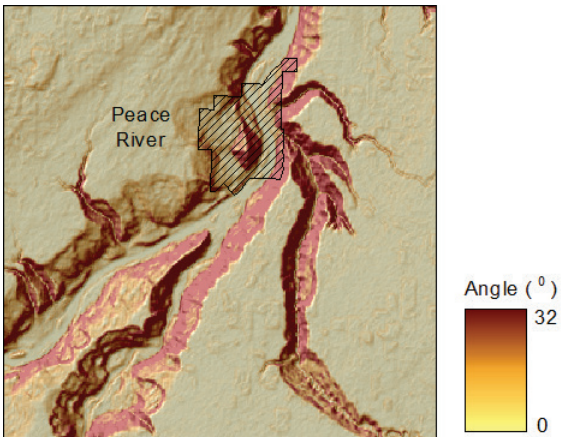


**Figure 14. Slope angle.**

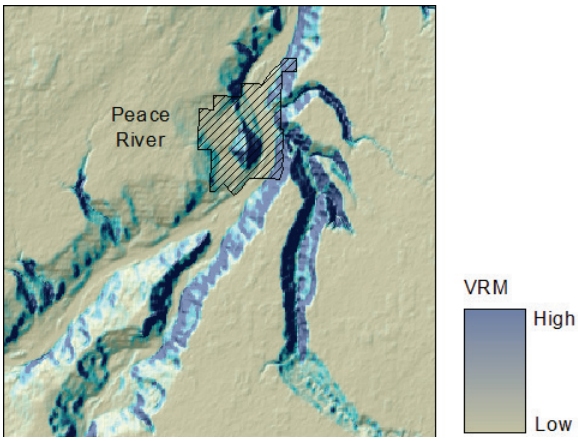


**Figure 15. Vector Ruggedness Measure.**

### *3.2.2 Regional Terrain Morphology*

Regional morphometric variables quantify landscape-scale topographic relationships. Topographic openness (Yokoyama et al., 2002) was used to visualize regional topographic convexities and concavities (Figure 16). In the context of landslide susceptibility, topographic openness is related to the maturity of river valleys and gullies, which often represent the foci of landslide activity. The relative slope position of the landscape was also calculated based on the ratio of the SRTM DEM elevation to channel base levels and ridge heights, which results in an estimate of slope height and valley depth (Conrad et al., 2015). Slope height (Figure 17) is related to the driving forces of landslide activity due to the potential energy available for downslope movement. Conversely, valley depth (Figure 18) quantifies the degree of fluvial incision and is particularly relevant for predicting the landslide susceptibility of incised river valley walls.

### *3.2.3 Topographic Wetness*

The topographic wetness index (TWI) (Figure 19) is a standard calculation for estimating the spatial distribution of soil moisture, based on the upslope contributing area of the DEM and the local slope angle (Boehner and Selige, 2006). The TWI provides an estimation of relative moisture in the upper part of the soil profile, and is commonly used as a predisposing factor in landslide susceptibility assessments. Low-relief components of the landscape are typically dominated by high TWI values (wetter surface conditions), and higher-relief landscape components are characterized by lower TWI values (drier surface conditions).

### *3.2.4 Physiography and Climate*

Fluvial processes and climate represent important agents in landslide susceptibility. River erosion increases landslide susceptibility by undercutting (and thus steepening) valley slopes as a result of meander bend propagation or channel incision. Climate influences landslide susceptibility because large precipitation differences occur across Alberta. This influences slope stability because water saturation reduces the cohesion of surficial and bedrock materials. An example of this occurs in the Upper Cretaceous Horseshoe Canyon Formation which comprises a succession of mudstone, sandstone, carbonaceous shales, and bentonite, which in the Edmonton region is highly landslide-prone (Rutter et al., 1998). However, these units are more stable in southeastern Alberta because the climate is more arid. Climate and precipitation were incorporated into the model by calculating the distance to major river features, and by using the average annual precipitation record over a 50-year period provided by Alberta Agriculture and Forestry.

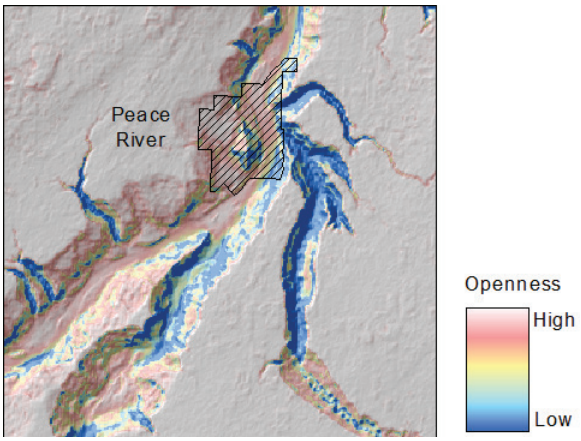


**Figure 16. Topographic openness.**

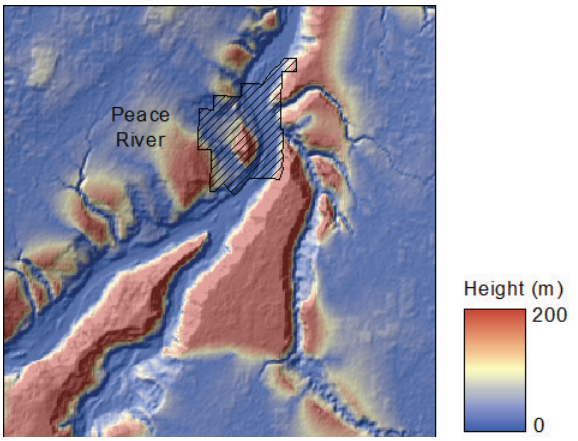


**Figure 17. Slope height.**

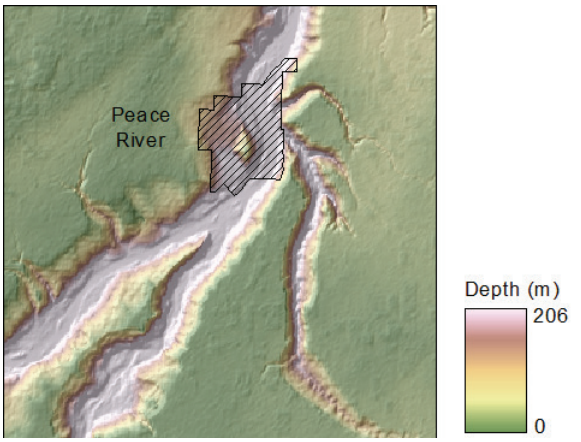


**Figure 18. Valley depth.**

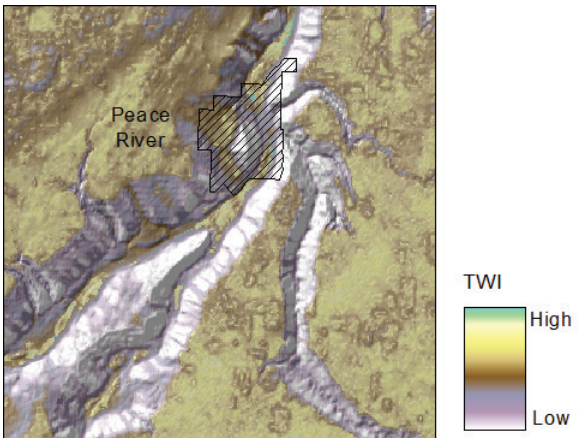


**Figure 19. Topographic wetness index.**

### 3.2.5 Surficial Geology

Regional geological conditions are one of the most important factors in landslide susceptibility because geology governs the lithology and mechanical properties of rock and sediment. The *Surficial Geology of Alberta* (Fenton et al., 2013a,b) was used to evaluate the role of surface and near-surface sediment types in the landslide susceptibility assessment. Thirteen genetically-defined classes that are present across the Alberta Plains (Figure 20) were used to describe the general surface material characteristics. The thickness of these surface and near-surface sediments is also an important factor in landslide susceptibility, with zones of landslide-prone terrain occurring in regions characterized by thicker sediments, e.g., in areas underlain by infilled palaeovalleys (Miller, 2000; Miller and Cruden, 2002; Morgan et al., 2012). Data derived from a geostatistical estimation of sediment thickness (MacCormack et al., 2015; Figure 21) was therefore used in the susceptibility model.

### 3.2.6 Bedrock Geology

The contribution of bedrock geology to landslide susceptibility was assessed by reclassifying the bedrock geological units of Alberta from Prior et al. (2013) into five classes of relative rock strength (Table 2; Figure 22) based primarily on the long-established relationship between landslide-prone strata and the depositional environment of geological formations in Alberta (e.g., Thomsen and Morgenstern, 1977). In general, high-energy depositional environments result in stronger coarse-grained formations while low-energy depositional environments result in weaker fine-grained formations. The relationship between depositional environment, lithology, and rock strength is complex for formations in which there is significant lithologic variability (e.g., alluvial systems comprised of intercalated sandstone and mudstone units). Therefore, strength classifications were made by considering the bulk characteristics of a formation as a whole. Bedrock strength classifications were reviewed by geologists with significant familiarity with each formation. Where necessary, classifications were adjusted to reflect formational properties

**Table 2. Ranking of the bedrock units based on bulk rock strength.**

| Bulk Rock Strength Ranking | Geological Region | Bedrock Unit |
|---|---|---|
| Low | Plains | Bearpaw Fm., Bluesky Fm., Clearwater Fm., Fish Scales Fm., Belle Fourche Fm., Joli Fou Fm., Kaskapau Fm., Lea Park Fm., Loon River Fm., Muskiki Fm., Pakowki Fm., Puskwaskau Fm., Second White Specks Fm., Carlile Fm., Niobrara Fm., Shaftesbury Fm., Spirit River Fm., Westgate Fm. |
| Medium-Low | Plains | Banff Fm., Belly River Gp., Coalspur Fm., Dinosaur Park Fm., Dunvegan Fm., Eastend Fm., Foremost Fm., Fort Vermilion Fm., Frenchman Fm., Grand Rapids Fm., Horseshoe Canyon Fm., Ireton Fm., McMurray Fm., Oldman Fm., Peace River Fm., Pelican Fm., Prairie Evaporite Fm., Ravenscrag Fm., Scollard Fm., Wabiskaw Member, Wapiti Fm., Watt Mountain Fm., Willow Creek Fm. |
| Medium | Plains | Contact Rapids Fm., lower Belly River Gp., Milk River Fm., Paskapoo Fm., Porcupine Hills Fm., St. Mary River Fm. |
| Medium-High | Plains | Blood Reserve Fm., Chinchaga Fm., Cooking Lake Fm., Cypress Hills Fm., Del Bonita gravel, Elk Point Gp., Grosmont Fm., Hand Hills Fm., Hay River Fm., Keg River Fm., Muskeg Fm., Slave Point Fm., Tathlina Fm., Twin Falls Fm., upland gravel, Waterways Fm. |
| High | Shield | Andrew Lake Granodiorite, Arch Lake Granitoid, Burntwood Complex, Charles Lake Granitoid, Chipewyan Granite, Colin Lake Granitoid, Fair Point Fm., Fishing Creek Granodiorite, Francis Granite, La Butte Granodiorite, Lazenby Lake Fm., Locker Lake Fm., Manitou Falls Fm., Marguerite River Complex, Otherside Fm., Rutledge River Complex, Slave Granitoid, Smart Fm., Taltson Basement Complex, Thesis Lake Granite, Waugh Lake Complex, Wolverine Point Fm., Wylie Lake Granodiorite |

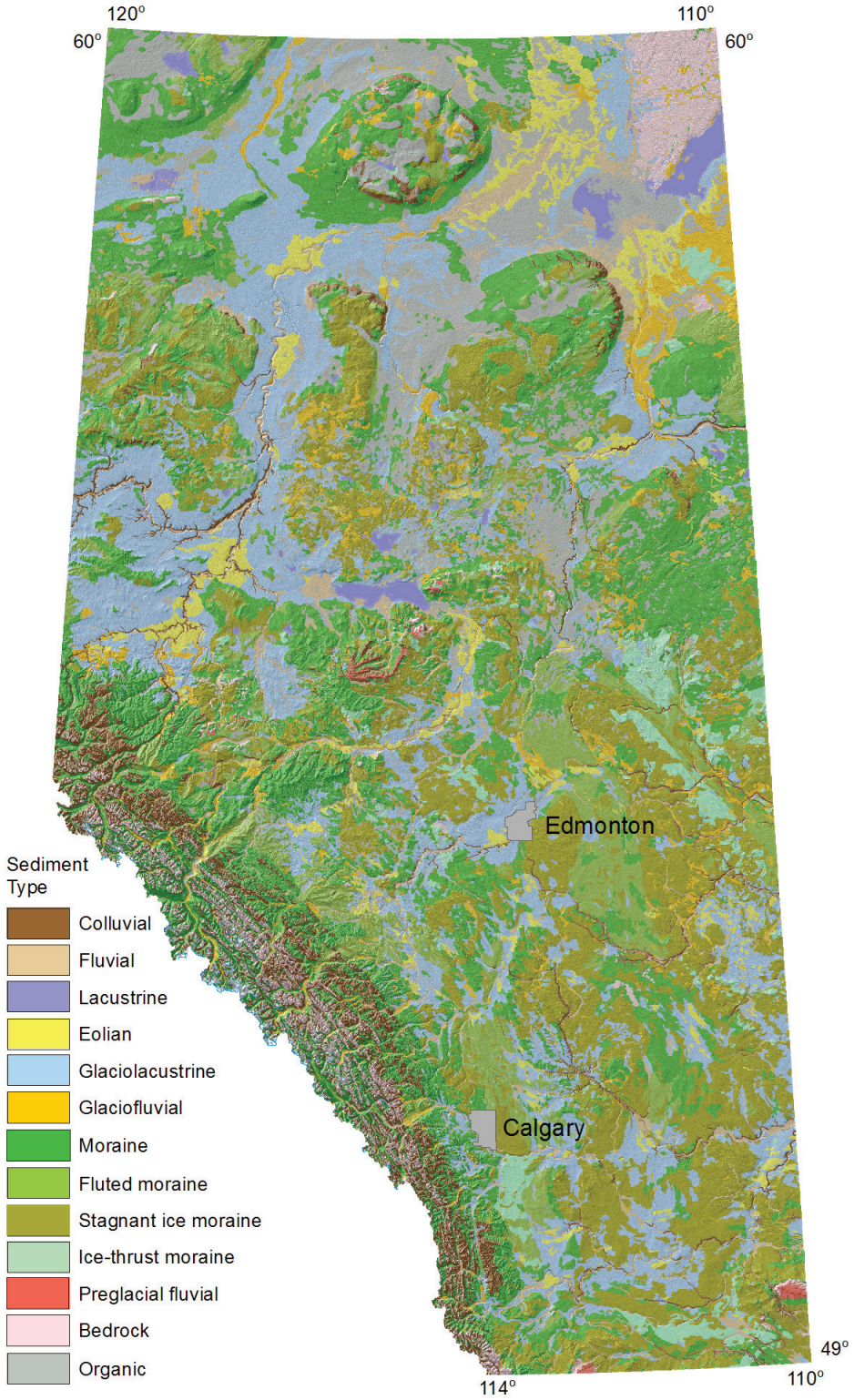


**Figure 20. Surficial geology (Fenton et al., 2013).**

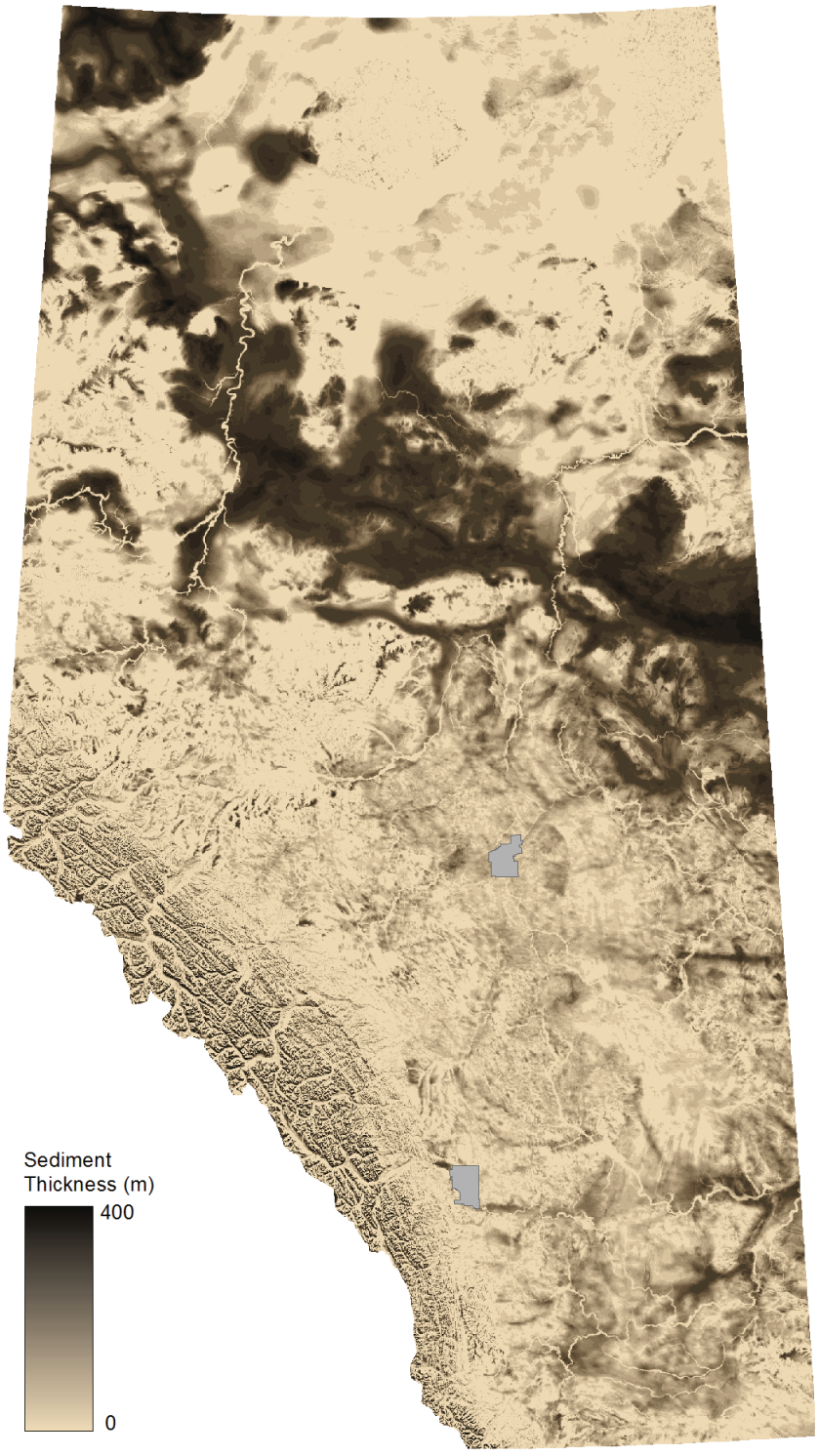


**Figure 21. Sediment thickness (MacCormack et al., 2015).**

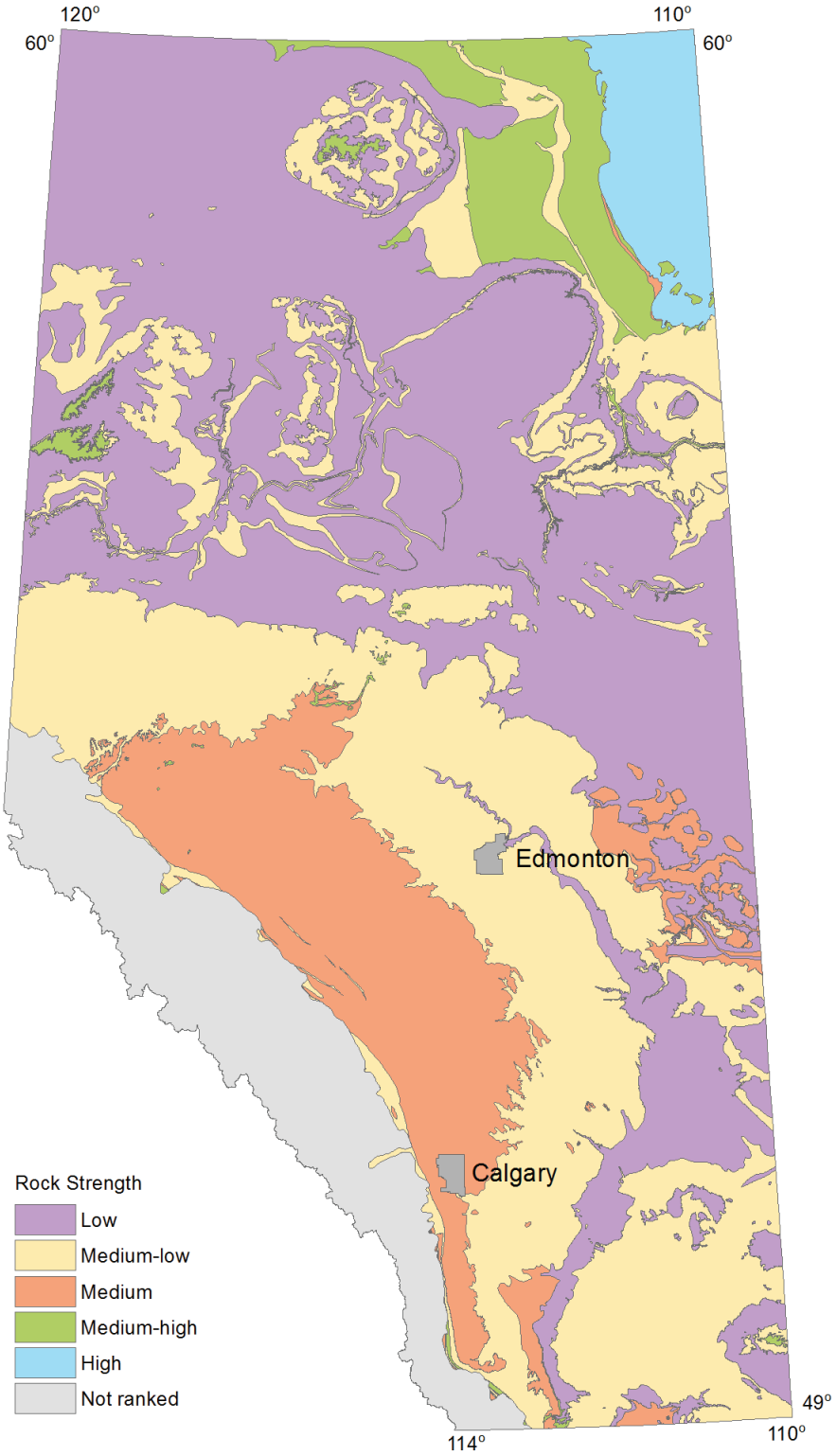


**Figure 22. Generalized bulk rock strength of bedrock units.**

beyond depositional environment and constituent lithology. In addition, the potential influence of bedrock structure on these rock properties was included in the analysis by calculating a raster of Euclidian distances to linear structural elements as mapped in the *Bedrock Geology of Alberta* (Prior et al., 2013).

### *3.2.7 Modelling Procedure*

#### 3.2.7.1 Stochastic Gradient Boosting model for predicting relative landslide susceptibility

A predictive modelling method termed Stochastic Gradient Boosting (Friedman, 2002) was used for the landslide susceptibility assessment. Stochastic Gradient Boosting uses a decision-tree structure to map how the occurrence of landslides relates to thresholds in the predisposing factors (e.g., slope, aspect, bedrock geology) using a hierarchy of splits and branches. The terminus of the branches, termed leaves, represents the class labels (i.e., landslide or non-landslide). Data from the landslide inventory represent the landslide cells that were used to train the model. The non-landslide cells were obtained by simple random sampling of the background geological, physiographic, and climatic conditions. The landslide susceptibility estimation represents the probability of membership in either the landslide or non-landslide classes. This probability is derived from the portion of instances where the predicted class was correct in each leaf, which is evaluated for every grid cell within the model. Unlike a single decision tree, the Stochastic Gradient Boosting algorithm improves prediction accuracy based on an additive process where additional decision trees are created to model observations that were not accurately predicted by the previous tree. At each iteration, the algorithm determines the gradient in which it needs to improve the modelled fit to the data, and selects a particular model that is in most agreement with the direction, i.e., the algorithm iteratively fits the model to the residuals. The final model represents a weighted average of the decision-tree ensemble.

#### 3.2.7.2 Model Uncertainty and variability

Model accuracy was assessed using a bootstrapping procedure with an ensemble of 20 model replications. These models were constructed by random sampling of the landslide and non-landslide grid cells. For each model replication, 75% of the mapped landslide cells were randomly drawn from the total population and were used to train the model, and the remaining 25% of landslide cells were used to validate the accuracy of the prediction. The final susceptibility map represents the mean of the 20 replicate models. The mean prediction uncertainty is provided in Table 3. The bootstrapping procedure also allows the sampling uncertainty to be visualized geographically, and the standard deviation of the model replicates was chosen as the uncertainty interval (Figure 23). Regions with the lowest uncertainty (less than 5%) occur in the plains and lowlands of the province, or in deeply incised valleys, where the distribution of landslides are well explained by topographic and geological factors. Regions with the highest uncertainty (up to ~25%) occur in some regional uplands including the Porcupine Hills (Figure 24). The higher uncertainty in these regions is due to the distribution of landslides being controlled by predisposing factors that are not evaluated in the model, such as localized geological, geotechnical, or hydrogeological conditions. These conditions may include structurally weak geological strata, or in the case of the Porcupine Hills, more steeply dipping bedding planes that occur near the western margin of the upland (Jackson, 1995).


**Figure 23. Predictive uncertainty.**

**Table 3. Mean prediction uncertainty.**

| | AUC | TPR | TNR | Accuracy | Kappa |
|---|---|---|---|---|---|
| **Mean** | 96.6% | 93.1% | 90.1% | 91.6% | 83.3& |
| **Std. Dev.** | 0.4% | 0.6% | 1.0% | 0.7% | 1.4% |

**AUC** (area under curve): the area under the receiver operating characteristic curve is based on the ratio of true positives to false positives.

**TPR** (true positive rate): the proportion of known landslide cells in the model that are correctly classified as having a high susceptibility.

**TNR** (true negative rate): the proportion of non-landslide cells in the model that are correctly classified as having a low susceptibility.

**Accuracy**: the overall proportion of correctly classified cells.

**Kappa**: the proportion of correctly classified cells after removing what would be obtained by chance selection.

# 4 Relative Landslide Susceptibility of the Alberta Plains

The Stochastic Gradient Boosting model indicates landslide susceptibility across the Alberta Plains is typically associated with areas of higher relief such as valley walls and the flanks of plateaus and uplands (Figure 24). Lower relief areas such as plains and lowlands, broad river terraces and floodplains are generally less susceptible. Although quite rugged, the Canadian Shield region of northeastern Alberta is not landslide susceptible due to the competent bedrock and thin sediment cover across this region.

The walls of major river valleys and their tributaries comprise the longest contiguous zones of landslide-susceptible terrain across Alberta. These zones are relatively narrow (typically <1 km wide) but can extend along one or both valley walls for 10s to 100s of kilometres. Wider zones of landslide-susceptible terrain (up to 2 km) occur within the western part of the Peace River valley which, at up to 250 m deep, represents Alberta's most deeply incised valley (Figure 25). Widespread, contiguous zones of landslide-susceptible terrain occur along steep slopes flanking relatively un-dissected plateaus including: the Caribou Mountains, Birch Mountains, Buffalo Head Hills, and the western Clear Hills (Figure 26). These zones may be 10s of kilometres long, up to 6 km wide, and up to 500 m in height. Less contiguous zones of landslide-susceptible terrain occur across heavily dissected plateaus or rugged uplands including: the Swan Hills, Grand Cache Benchland, Summit Benchland, Cypress Hills, the eastern Clear Hills and Porcupine Hills (Pettapiece, 1986; Figure 27). Collectively however, landslide-susceptible terrain in these dissected regions is extensive.

## 4.1 Significance to the Geomorphology, History, and Development of Alberta

Landslides are part of the geomorphic evolution of the plains landscape which, post-Paleocene, has been dominated by denudation (Nurkowski, 1984; Osborn et al., 2006). Landslides contribute to denudation by progressively removing plateaus and uplands, and widening river valleys. Although a natural process, landslides are disruptive from a human perspective as they can damage infrastructure and render land unsuitable for development unless mitigative measures are put in place. At a provincial scale, landslide-susceptible terrain exerts a significant influence on land-use and development patterns, particularly across regions where development is concentrated, such as along the routes of major rivers where they are incised within plains and lowland regions (Pettapiece, 1986).

Landslide-susceptible terrain along valley walls presents a particular challenge to two types of development: linear infrastructure (roads, rail lines, pipelines) and urban development. Routing of linear infrastructure around these zones is often impractical. As a result, route planners are typically required to assess landslide hazard within susceptible zones in order to locate suitable crossings, and potentially to

implement mitigative measures. Within urban areas, which often radiate from historical developments on major rivers (e.g., Edmonton, Calgary, Lethbridge, Ft. McMurray, Peace River, Athabasca, and Medicine Hat), contiguous zones of landslide-susceptible terrain may restrict development and compartmentalize the city. Development within landslide-susceptible terrain is impacted not only during planning and construction stages, but throughout the lifespan of the development as slope movement, or the potential thereof, typically necessitates monitoring, mitigation, or repair.

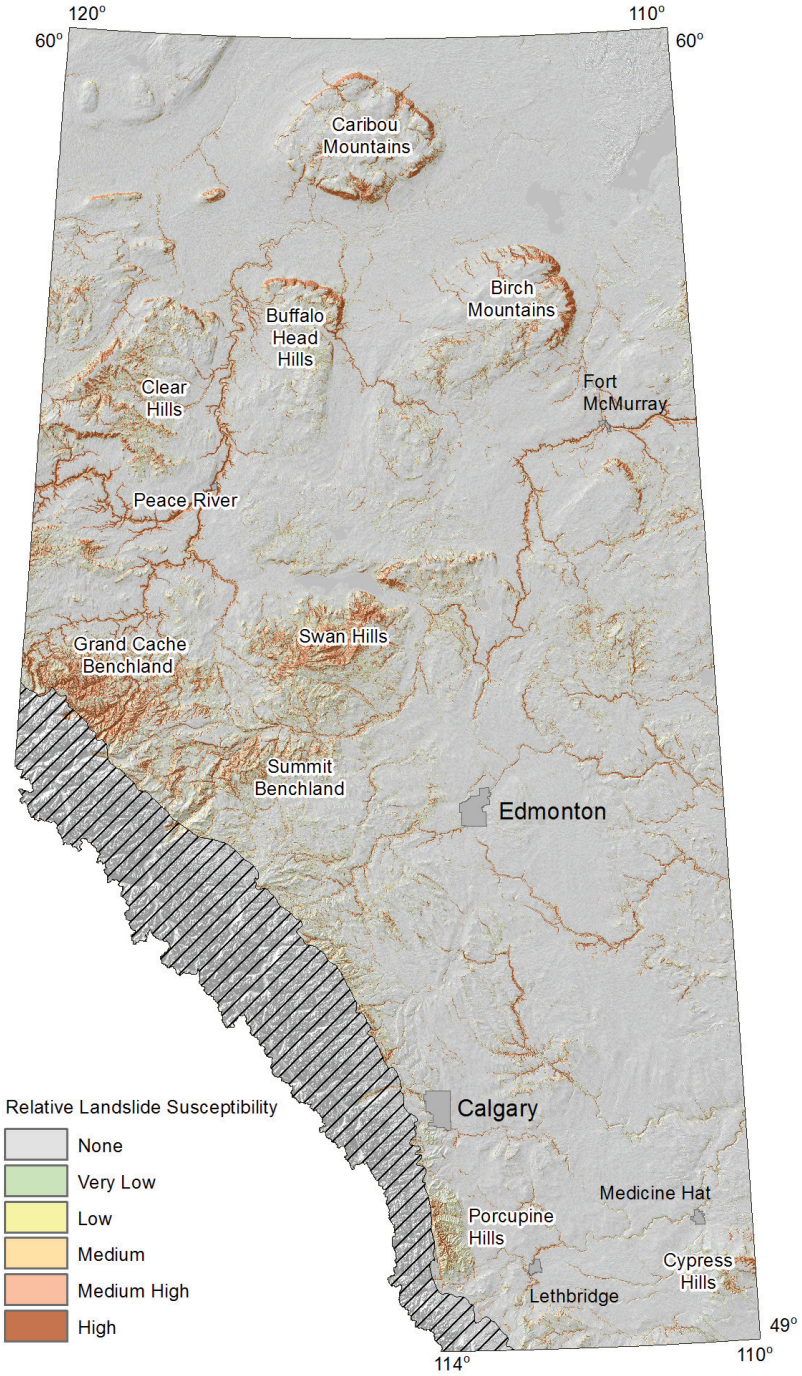


**Figure 24. Areas of relatively high landslide susceptibility.**

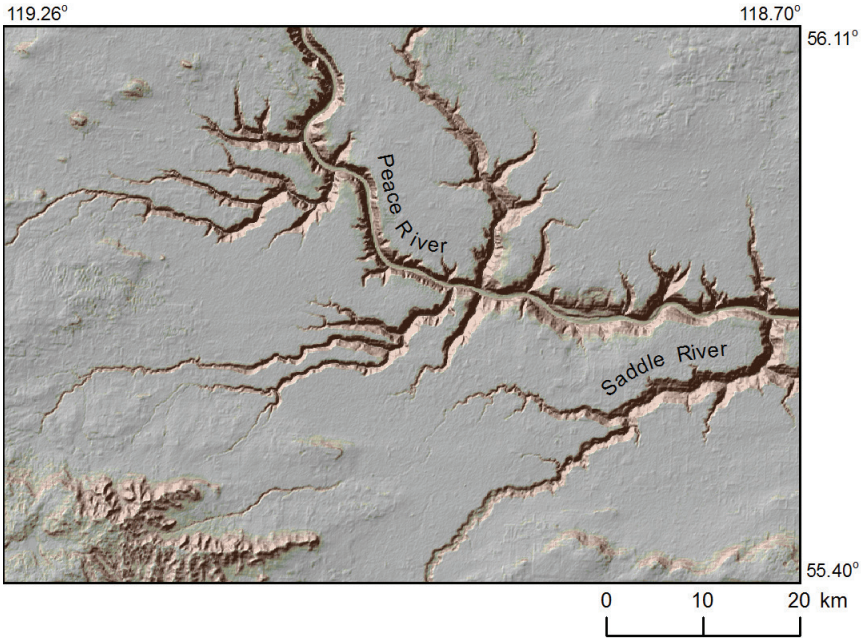


**Figure 25. Contiguous zones of landslide-susceptible terrain along the Peace and Saddle rivers and their tributaries.**

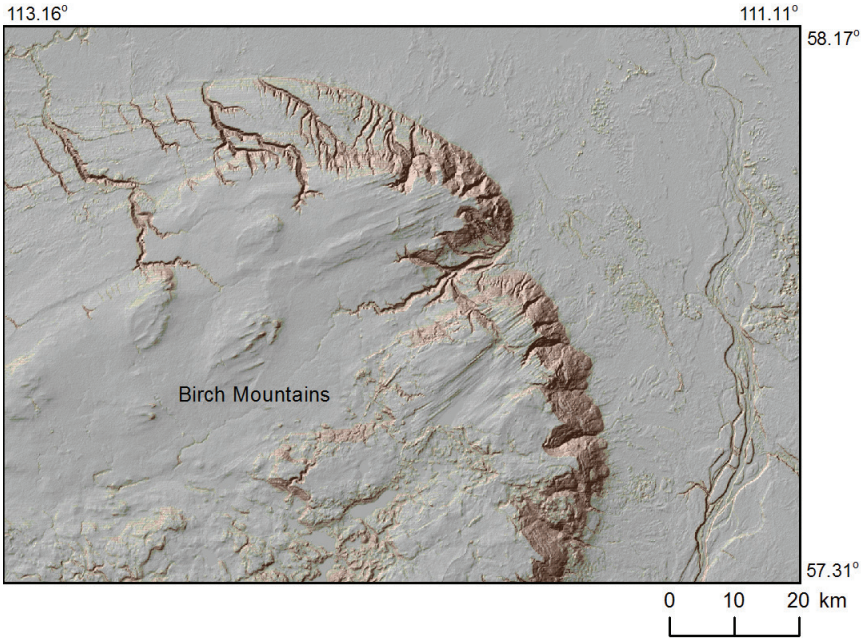


**Figure 26. A broad zone of landslide-susceptible terrain on the east flank of the Birch Mountains upland.**

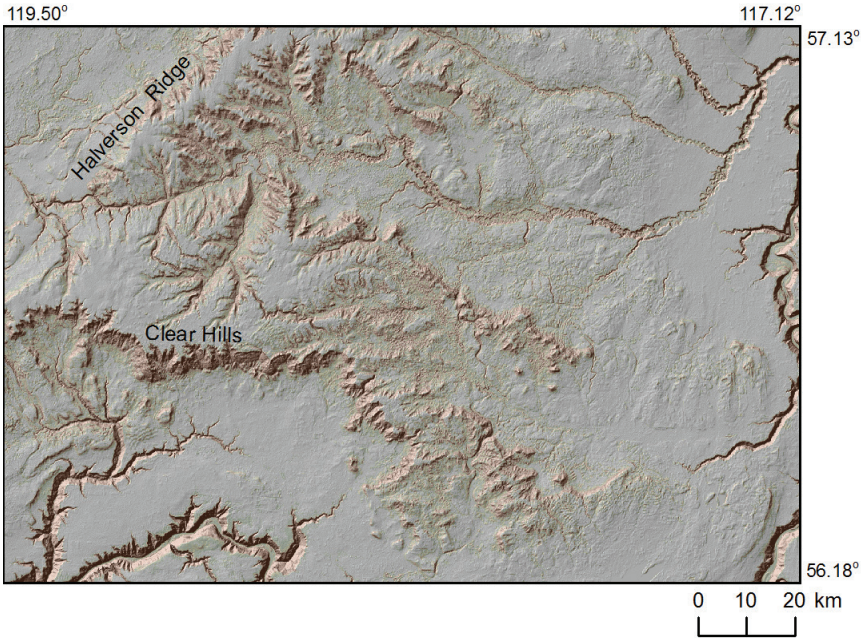


**Figure 27. Discontinuous zones of landslide-susceptible terrain distributed across the eastern portions of the Clear Hills and Halverson Ridge.**

# 5 References


Barlow, J.P. (2000): Slope movement patterns in young valley slopes in Northern Alberta, Canada; *in* Landslides in Research, Theory and Practice, Thomas Telford, London, p. 113-120.

Boehner, J. and Selige, T. (2006): Spatial prediction of soil attributes using terrain analysis and climate regionalisation; *in* SAGA - analysis and modelling applications, Goettinger Geographische Abhandlungen, v. 115, p. 13-27.

Bostock, H.S. (2014): Physiographic regions of Canada (2nd edition); Geological Survey of Canada, "A" Series Map 1254A, scale 1:5 000 000.

Brabb, E.E. (1984): Innovative approaches to landslide hazard and risk mapping; Proceedings of the 4th International Symposium on Landslides, Toronto, Ontario, Canada, v. 1, p. 307–324.

Conrad, O., Bechtel, B., Bock, M., Dietrich, H., Fischer, E., Gerlitz, L., Wehberg, J., Wichmann, V. and Boehner, J. (2015): System for Automated Geoscientific Analyses (SAGA) v. 2.1.4.; Geoscientific Model Development, no. 8, p. 1991-2007.

Cruden, D.M. (1991): A simple definition of a landslide; Bulletin of the International Association of Engineering Geology, no. 43, p. 27-29.

Cruden, D.M., Keegan, T.R. and Thomson, S. (1993): The landslide dam on the Saddle River near Rycroft, Alberta; Canadian Geotechnical Journal, v. 30, p. 1003-1015.

Cruden, D.M. and Varnes, D.J. (1996): Landslides types and processes; *in* Landslides: investigation and mitigation, Transportation Research Board, National Academy of Science, Special Report 247, Washington, District of Columbia, p. 36–75.

Fenton, M.M., Waters, E.J., Pawley, S.M., Atkinson, N., Utting, D.J. and Mckay, K. (2013a): Surficial geology of Alberta; Alberta Energy Regulator, AER/AGS Map 601, scale 1:1.000 000.

Fenton, M.M., Waters, E.J., Pawley, S.M., Atkinson, N., Utting, D.J. and Mckay, K. (2013b): Surficial geology of Alberta: ungeneralized digital mosaic (GIS data, polygon features); Alberta Energy Regulator, AER/AGS DIG 2013-0001.

Friedman, J.H. (2002): Stochastic gradient boosting; Computational Statistics and Data Analysis, v. 38, no. 4, p. 367-378.

Highland, L.M. and Bobrowsky, P. (2008): The landslide handbook - a guide to understanding landslides; United States Geological Survey, Circular 1325, 129 p.

Hungr, O., Evans, S.G., Bovis, M.J., Hutchinson, J.N. (2001): A review of the classification of landslides of the flow type; Environmental and Engineering Geoscience, v. 7, no. 3, p. 221-238.

Jackson, L.E., Jr. (1995): Quaternary geology and terrain inventory, Eastern Cordillera NATMAP project. Report 1: regional landslide characterization; Current Research, v. 1995-A, p. 159-166.

Jackson, L.E., Jr. (2002): Landslides and landscape evolution in the Rocky Mountains and adjacent Foothills area, southwestern Alberta, Canada; Geological Society of America Reviews in Engineering Geology, v. 15, p. 325-344.

MacCormack, K.E., Atkinson, N. and Lyster, S. (2015): Sediment thickness of Alberta, Canada; Alberta Energy Regulator, AER/AGS Map 603, scale 1:1 000 000.

Miller, B.G.N. (2000): Two landslides and their dams, Peace River Lowlands, Alberta. M.Sc. thesis, University of Alberta, 149 p.

Miller, B.G.N. and Cruden, D.M. (2002): The Eureka River landslide and dam, Peace River Lowlands, Alberta; Canadian Geotechnical Journal, v. 39, no. 4, p. 863-878.

Mollard, J.D. (1977): Regional landslide types in Canada; Engineering Geology, v. 3, p. 29-56.

Morgan, A.J., Paulen, R.C., Slattery, S.R. and Froese, C.R. (2012): Geological setting for large landslides at the Town of Peace River, Alberta (NTS 84C); Energy Resources Conservation Board, ERCB/AGS OFR 2012-04, 33 p.

Nurkowski, J.R. (1984): Coal quality, coal rank variation and its relation to reconstructed overburden, Upper Cretaceous and Tertiary plains coals, Alberta, Canada; American Association of Petroleum Geologists Bulletin, v. 68, no. 3, p. 285–295.

Osborn, G., Stockmal, G. and Haspel, R. (2006): Emergence of the Canadian Rockies and adjacent plains: a comparison of physiography between end-of-Laramide time and the present day; Geomorphology, v. 75, no. 3-4, p. 450–477.

Parise, M. (2001): Landslide mapping techniques and their use in the assessment of the landslide hazard; Physics and Chemistry of the Earth, Part C: Solar, Terrestrial and Planetary Science, v. 26, no. 9, p. 697-703.

Pawley, S.M., Hartman, G.M.D. and Chao D.K. (2016): Relative landslide susceptibility model of the Alberta Plains and shield regions; Alberta Energy Regulator, AER/AGS Map 605, scale 1:1 000 000.

Pettapiece, W.W. (1986): Physiographic subdivisions of Alberta; Land Resources Research Centre, Research Branch, Agriculture Canada, scale 1:1 500 000.

Prior, G.J., Hathway, B., Glombick, P.M., Pană, D.I., Banks, C.J., Hay, D.C., Schneider, C.L., Grobe, M. Elgr, R. and Weiss, J.A. (2013): Bedrock geology of Alberta; Alberta Energy Regulator, AER/AGS Map 600, scale 1:1 000 000.

Rutter, N.W., Andriashek, L.D., Stein, R. and Fenton, M.M. (1998): Engineering geology of the Edmonton area; *in* Urban geology of Canadian cities, Geological Association of Canada, Special Report 42, p. 71-92.

Sappington, J.M., Longshore K.M. and Thomson, D.B. (2007): Quantifying landscape ruggedness for animal habitat analysis: a case study using bighorn sheep in the Mojave Desert; Journal of Wildlife Management v. 71, no. 5, p. 1419 -1426.

Soe Moe, K.W., Cruden, D.M., Martin, C.D., Lewycky, D. and Lach, P.R. (2009): Mechanisms and kinematics of river valley landslides in Edmonton. Annual Conference of the Transportation Association of Canada, Vancouver, British Columbia.

Sauchyn, D.J. and Nelson, H.L. (1999): Origin and erosion of the Police Point landslide, Cypress Hills, Alberta; *in* Holocene climate change and environmental change in the Palliser Triangle: a geoscientific context for evaluating the impacts of climate change on the southern Canadian Prairies, D.S. Lemem and R.E Vance (ed.); Geological Survey of Canada Bulletin, v. 534, no. 295, p. 257-265.

Thomsen, S. and Morgenstern, N.R. (1977): Factors affecting distribution of landslides along rivers in southern Alberta; Canadian Geotechnical Journal, v. 14, no. 4, p. 508-523.

U.S. Geological Survey (2004): Landslide type and processes; fact sheet 2004-3072, URL http://pubs.usgs.gov/fs/2004/3072/fs-2004-3072.html [July 2004].

U.S. Geological Survey (2014): Shuttle Radar Topography Mission digital elevation model data (1-arc second resolution); Earth Resources Observation and Science Center, URL http://earthexplorer.usgs.go [January 2015].

Yokoyama, R., Shirasawa, M. and Pike, R.J. (2002): Visualizing topography by openness: A new application of image processing to digital elevation models; Photogrammetric Engineering and Remote Sensing, v. 68, no. 3, p. 257-265.